Journal of Applied Mechanics Vol.13, pp.683-690 (August 2010) JSCE

An Inversion Scheme to Improve the Accuracy of Earthquake Source Parameters using Multiscale Approach with Finite Element Method

Pher Errol B. Quinay*, Satoshi Noguchi*, M.L.L.Wijerathne**, Tsuyoshi Ichimura**, Muneo Hori**

*Department of Civil and Environmental Engineering Tokyo Institute of Technology
(2-12-1 Ookayama, Meguro-ku, Tokyo 152-8550)
**Earthquake Research Institute, The University of Tokyo
(1-1-1 Yayoi, Bunkyo-ku, Tokyo 113-0032)

The crust structure and earthquake source parameters are known to strongly influence the ground motions at the surface. Thus, the accuracy of these parameters is important to predict the ground motion that is essential in engineering analysis. Recently, an inversion scheme has been proposed[1] that aims to estimate the crust structure with accuracy up to 1.0 Hz target frequency. In the present paper, an inversion scheme is proposed which aims to improve the accuracy of earthquake source parameters from low frequency to high frequency (up to 1.0 Hz). Both studies take advantage of a sophisticated code implementation of the Finite Element Method to accurately compute synthetics. Promising results have been obtained for future application to simultaneous inversion of crust structure and earthquake source parameters.

Key Words : *hybrid-grid FEM, source parameter estimation, multiscale approach*

1. Introduction

The prediction of the strong ground motion with high accuracy plays an important role for disaster mitigation, formulation of effective countermeasures, and enforcement of policy against large-scale earthquake disaster. Since earthquake motion is strongly influenced by the nature of the seismic source and the upper crust which has complex velocity structure, their accurate estimation is important in order to improve the understanding of their mechanism and contribute in predicting the strong ground motion with high accuracy. Researches to clarify the detailed structure and property of fault plane, and to build accurate three-dimensional (3D) crust structure model, were conducted extensively in Tokyo and Osaka metropolitan districts where a predicted large-scale earthquake can have a significant impact on normal social activities[2)3)]. However, the accuracy of available 3D crust structure models is verified only for a very low frequency range ($f \leq 0.20$ Hz)[2)], which is not sufficient to account for higher frequencies that affect the response of large-scale civil structures on the ground surface. Recently, a numerical study presented a scheme that takes advantage of the accurate modeling capability of the Finite Element Method to estimate 3D crust layer boundary for up to 1.0 Hz frequency [1)]. This study assumes that source parameters accurate up 1.0 Hz frequency are available.

With regards to source parameter estimation, the use of horizontally-layered velocity structure leads to accuracy of results that are not sufficient for use in engineering applications, such as in seismic analysis of large-scale structures. Recognizing the importance of higher frequencies, new inversion studies based on theoretical, empirical, or combination of both, that utilize detailed information from geophysical exploration and GIS (among others), and targeted higher accuracies ($f \leq 3.0$ Hz), have been conducted. Examples of these studies are [4),5)].

In our study, we perform a numerical study on improving the accuracy of source parameters to higher frequencies using the same numerical tools used in [1)]. We assume that the accuracy of available crust structure is up to the same order of accuracy as to the accuracy we aim for source parameters. At this stage, we perform only source parameter[6)] inversions, but since the methodology is similar to [1)], integrating the two methods in the future, as in simultaneous inversion is intended. In this study, we present the scheme to estimate the following earthquake source parameters: point source location, magnitude, rise time, and moment tensors. In comparison with existing source parameter estimation methods, this scheme is based on a combination of (1) a hybrid-grid FEM[7] that can automatically-generate finite element (FE) models and calculate synthetics, and (2) a multiscale approach that repeats inversion from low target frequency to high target frequency.

This paper is divided as follows: Section 2 describes the forward modeling tool. The background formulation is first shown and then the applicability to actual problem settings is demonstrated. In Section 3, we introduce the proposed inversion method for source parameter estimation. A numerical experiment on each parameter is carried out to check the applicability of our proposed scheme and at the same time, study the behavior of target parameters. In the end, we discuss the possible extensions of this study.

2. Hybrid-grid FEM as the forward modeling tool

It is known that obtaining good results in inversion relies on accurate calculation of sensitivities. Our study uses a sophisticated implementation of the FEM, the Multi-resolution Structured and Unstructured Grid FEM (MCFEM)[7], for forward modeling. This section demonstrates the applicability of this tool in handling an actual problem - an observed earthquake in Kanto region. We demonstrate its capability to model actual domain features, such as topography and irregular layering. We aim to reproduce the surface-recorded ground motions in several observation stations near the target domain.

Methodology

Assuming the target crust as elastic body, the equation of elastodynamics as shown below is used.

$$(c_{ijkl}u_{k,l})_{,i} + f_j = \rho \ddot{u}_j. \tag{1}$$

Therein, $c_{ijkl},\ u_j,\ \rho,\ (\dot{\ }),\ (\ )_{,j},\ and\ f_j$ are component of heterogeneous elastic tensor, displacement at j direction, density, time differentiation, spatial differentiation for j direction, and external forces at j direction, respectively.

Galerkin discretization in space by finite elements is applied to Eq.(1), and a damping term that is proportional to the velocity is added to this equation.

$$\mathbf{Ku} + \mathbf{Cv} + \mathbf{Ma} = \mathbf{f}. \tag{2}$$

Therein, $\mathbf{K}$, $\mathbf{M}$, $\mathbf{u}$, $\mathbf{v}$, $\mathbf{a}$, and $\mathbf{f}$ are stiffness matrix, mass matrix, displacement vector, velocity vector, acceleration vector, and force vector, respectively. $\mathbf{C}$, is the Rayleigh damping computed as,

$$\mathbf{C} = \alpha\mathbf{M} + \beta\mathbf{K}, \tag{3}$$

where α and β are Rayleigh constants computed from this equation,

$$\frac{1}{2Q_k} = \frac{\alpha}{2\omega_k} + \frac{\beta\omega_k}{2}, \tag{4}$$

for the frequency range of interest. In Eq.(4), Q_k and ω_k are quality factor and natural frequency, respectively, associated with the k-th mode.

The Newmark β method ($\beta = 1/4$) is used for discretization of time domain.

$$\begin{aligned}&(\mathbf{K} + \frac{2}{\Delta t}\mathbf{C} + \frac{4}{\Delta t^2}\mathbf{M})\mathbf{u}^{n+1} = \\ &(\frac{2}{\Delta t}\mathbf{C} + \frac{4}{\Delta t^2}\mathbf{M})\mathbf{u}^n + (\mathbf{C} + \frac{4}{\Delta t}\mathbf{M})\mathbf{v}^n + \mathbf{Ma}^n + \mathbf{f}^{n+1}.\end{aligned} \tag{5}$$

A superscript n indicates the time step, and Δt indicates the time increment of analysis. Lumped mass matrix is applied for mass matrix.

The MCFEM can automatically generate a 3D model that has complicated crust structure with efficient use of computational resources[7]. We solve Eq.(5) using the preconditioned conjugate gradient method (PCG). The element by element (EBE) method was implemented so that the $\mathbf{K}$, $\mathbf{M}$, and $\mathbf{C}$ need not be assembled to global matrices. In doing so, we expect significant reduction in needed memory storage, and elliminated the resulting computational time of the matrix assembly. To treat the outgoing waves in the truncated boundary, viscous boundary [8] and absorption band[9] are applied to the sides and bottom surfaces of the model as absorbing boundary condition.

Numerical Verification of the MCFEM

In [7], the accuracy of the method is compared and verified with other FEM-based implementation for simple case problems. As demonstrated in the paper, the use of numerical techniques such as background cell and octree structure allowed for efficient handling of structured and unstructured grid elements as well as reduction of memory storage requirements. Lastly, the applicability of MCFEM for modeling realistic crust structure is detailed.

Application example of forward modeling method: Reproduction of observed earthquake

The observed earthquake in Kanto region is reproduced by 3D FE analysis. The results are compared with the observed earthquake motion at 10 seismic stations[10]. We use the mechanism solution estimated by National Research Institute for Earth Science and Disaster Prevention (NIED)[11] for the source parameter data. The mechanism solution of target observed earthquake is shown in **Table 1**. The rise time is estimated by the reference[12]. In addition, crust structure is modeled using a 3D Kanto crust data[13] ob-

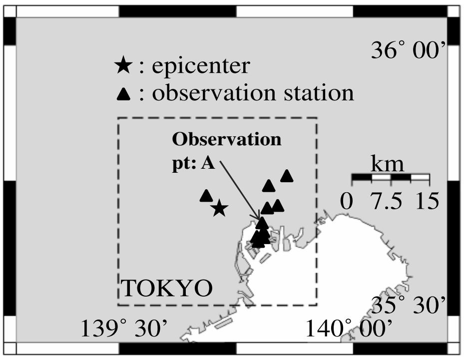

a) target region

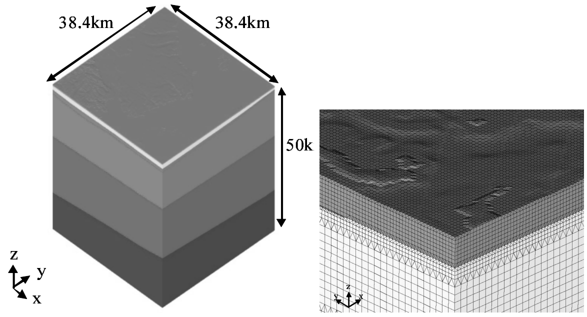

b) Kanto crust model b) generated mesh

Fig. 1 Target domain.

Table 1 Properties of target observed earthquake[11].

date:	2000.8.18
latitude:	35.7N
longitude:	139.7E
depth:	35km
strike, dip, rake:	59°, 74°, 65°
magnitude:	Mw3.8
rise time:	0.18 sec

Table 2 Material properties[13].

	ρ kg/m^3	V$_p$ m/s	V$_s$ m/s	Q
1st layer	1950	1850	500	60
2nd layer	2150	2560	1000	150
3rd layer	2300	3200	1700	200
4th layer	2700	5800	3360	500
5th layer	2800	6600	3700	600
6th layer	4400	8040	4480	800

tained from the Special Project for Earthquake Disaster Mitigation in Urban Areas[2]. The target domain is depicted by dotted line in **Fig. 1**a), and the size of domain is $38.4 \times 38.4 \times 50$km. The crust structure consists of six layers, and material properties of each layer, estimated by reference[13] are shown in **Table 2**. **Fig. 1**c),d) shows the numerical model automatically-generated by MCFEM using 3D Kanto crust data. The element size is set so that shear wavelengths corresponding to 1.0 Hz are resolved with 10 elements per wavelength. Eq.(5) is solved by PCG method with the convergence condition that the relative error is less than 10^{-6}.

An example of comparison of computed result with observed earthquake motion is shown in **Fig. 2**. This figure shows the velocity components of a waveform at EW, NS, and UD directions which are lowpass-filtered ($f \leq$1.0 Hz). The result in **Fig. 2** shows that the amplitude were reproduced with relatively good accuracy for all three components waveforms in Observation point A. Similar responses were observed in some other seismic stations. With these results, we can render the MCFEM suitable as a forward modeling tool in our inversion.

However, eventhough responses in some seismic station have good agreement, there were some disagreements in phase property and durations of ground motion, as can also be seen in **Fig. 2**. Assuming there are no errors in the waveform data, we can directly attribute the disagreements to the accuracy of the source mechanism and 3D crust structure used, in that for our problem: 1) the source mechanism is estimated by inversion analysis based on 10 to 100 sec range with assumption of horizontally-layered crust structure[11]; and 2) the accuracy of 3D crust model is verified only up to 0.2 Hz[2]. Thus, these suggest that the accuracy of source mechanism and crust structure model needs to be improved towards highly-accurate reproduction of approximately 1.0 Hz earthquake motion.

3. Waveform inversion to estimate earthquake source parameters

Many recent studies use theoretical and empirical Green's functions to estimate source parameters in low target frequencies ($\leq$1.0 Hz) and high target frequencies ($\geq$1.0 Hz)[4),5),14]. In our study, we define high target frequency as frequencies that are up to 1.0 Hz, and low frequencies as around 0.2 or 0.3 Hz. In the previous section, we learned that the velocity structure guaranteed up to 0.2 Hz can lead to disagreements in the comparison of waveforms in some seismic stations.

Many different numerical techniques to approach the global solution in an efficient manner have been presented (examples are [14),15]). In this study, we propose a new methodology based on the Finite Element Method (FEM) for calculating sensitivities, and a Quasi-Newton method for the minimization of the objective function. In inversions that calculates theoretical Green's functions as synthetics, the most commonly-used method is the FDM because it is fast, and modeling the source parameters can be

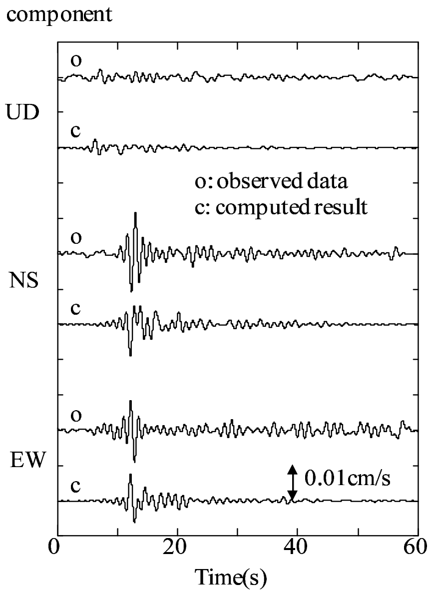

Fig. 2 Velocity waveform (in cm/s) at observation point, A,in reproduction of observed earthquake: Comparison of computed result with observed data

done with ease in the structured grid. However, FDM has difficulty in modeling domain features such as irregular layering and surface topography, and satisfying the surface traction-free condition is not as straightforward as in FEM. FEM is known to be computationally-expensive for use in inversions, but with the smart implementation of different numerical techniques (see [7]), it can perform much better than FDM, especially in models where complicated regions can significantly affect the results.

In this section, we present the details of the inversion procedure. Several numerical experiments on source parameter estimation by waveform inversion are conducted. Henceforth, the target surface response is called reference response, and the surface response which is solved using numerical analysis is called synthetic response. The inversion is conducted by solving optimization problem of minimizing residual of reference and synthetic response in unknown source parameter and known crust structure.

We calculate the synthetic response using MCFEM, and numerical analysis is conducted by solving Eq.(2) using PCG method, with the convergence condition that the relative error is less than 10^{-6}. The model is discretized in a hybrid grid, with tetrahedra and cubic element dimensions set to ten (10) elements per shear wavelength. The algorithm of the inversion is as follows:

Step 1:
Initialization of inversion parameters, x_k. ($k = 0$)
Step 2:
Generate synthetic model by the parameters at k-th iteration.
Step 3:
Conduct forward modeling and obtain synthetic response.
Step 4:
Solve the optimization problem and update the parameters as x_{k+1}.
Step 5:
If the solution meets a termination criteria, the calculation is stopped.
Otherwise proceed to Step 6.
Step 6:
Returning to step 2 as $k = k + 1$.

For Step 4, to minimize the residual of reference and synthetic response, we use the objective function,

$$f(\mathbf{x}) = \sqrt{\frac{\sum_{r=1}^{NR}\sum_{i=1}^{3}\sum_{t=1}^{NT}(\tilde{u}_{it}(\mathbf{s}_r) - u_{it}(\mathbf{s}_r;\mathbf{x}))^2}{\sum_{r=1}^{NR}\sum_{i=1}^{3}\sum_{t=1}^{NT}(\tilde{u}_{it}(\mathbf{s}_r))^2}}. \tag{6}$$

Therein, $\mathbf{x}$, $\mathbf{s}$, NR, r, i, NT, t are: model parameter, receiver points, total number of receivers, receiver counter, spatial component, total time step, and time step counter, respectively. $\tilde{u}$ is the displacement vector of the reference waveform, and u is the displacement vector of synthetic waveforms.

In this study, the quasi-Newton method, Broyden-Fletcher-Goldfarb-Shanno (hereafter, BFGS) method[17], is used as optimization method to minimize Eq.(6). The BFGS is one of the most effective method for solving optimization problems, because it has the good global convergence property of steepest decent method and the fast local convergence property of Newton method. The same method is used on [1]

It is known that there is difficulty in obtaining the global minimum using high resolution model if the initial solution used is the solution estimated by a low resolution model. This is because earthquake response becomes more complex in high resolution model, and the solution tends to converge to a local minimum. To remedy this, the convergence to local minimum is prevented by repeating inversions using a model that satisfies accuracy from low to high spatial resolution in a series of steps. Such multiscale approach has been previously applied in recent inversion studies (examples are, [15] for dynamic source inversions, and [14] for low-frequency inversion in the determination of broadband seismic wave radiation process of the 2000 western Tottori, Japan earthquake). In our study, we implemented a straightforward multiscale approach that incrementally satisfies accuracy from low-spatial resolution to high-spatial resolution. An important characteristic of this approach is the targeting of frequency components where a param-

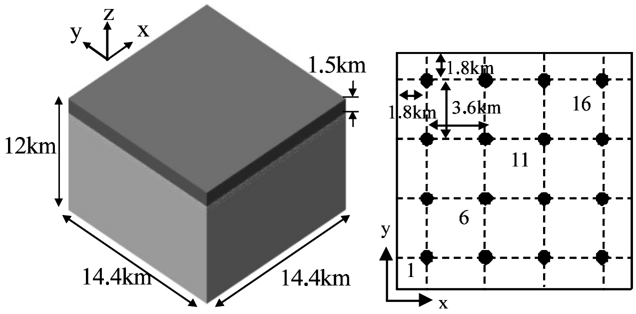

a) crust model b) observation points

Fig. 3 Model used for source inversion.

Table 3 Problem settings of fault inversion.

domain size:	-7.2 km $\leq$ x $\leq$ 7.2 km
	-7.2 km $\leq$ y $\leq$ 7.2 km
	-12.0 km $\leq$ z $\leq$ 0 km
1^{st}layer (thickness):	1.5 km
1^{st}layer:	ρ = 1900 kg/m^3
	V_p = 2300 m/sec
	V_s = 1500 m/sec
	Q_p = 100
	Q_s = 100
2^{nd}layer:	ρ = 2500 kg/m^3
	V_p = 4500 m/sec
	V_s = 3000 m/sec
	Q_p = 300
	Q_s = 300
excitation:	M_0 (2 t^2/T_0^2) $0 \leq t \leq \frac{T_0}{2}$
	M_0 (1-2 $(t-T_0)^2/T_0^2$) $\frac{T_0}{2} \leq t \leq T_0$
	M_0 $t > T_0$

Table 4 Fault location inversion.

	x(m)	y(m)	z(m)
initial solution	2000	2000	-8000
inversion result	150	150	-5850
reference solution	150	150	-5850

eter or a group of parameters is sensitive. Knowing that different source parameters can be estimated with good accuracy at some specific range of frequencies (for example: moment tensors at very low frequency), we take advantage of this to reduce the ill-posedness of the inversion problem. Moreover, effort-wise, the advantage of using this approach is that a 3D FE analysis with low resolution model does not require much computational load as compared with a high resolution model. Thus, the over-all computation speed is also improved since inverse problems generally require many forward modeling iterations.

Table 5 Rise time and seismic moment inversion.

	rise time (sec)	seismic moment (Nm)
initial solution	1.5	1.5×10^{17}
inversion result	2.0	1.0×10^{17}
reference solution	2.0	1.0×10^{17}

Table 6 Moment tensor inversion.

	M_{11}	M_{22}	M_{12}	M_{13}	M_{23}
initial	0	0	0	0	1
final	-0.226	-0.034	-0.725	0.631	-0.127
reference	-0.225	-0.035	-0.725	0.631	-0.128

Application Example

In this part, the waveform inversion scheme to estimate source parameters in high resolution ($\leq$1.0 Hz) is verified. We aim to observe source parameter sensitivities, for a problem with a point source and assuming that the crust model is accurate up to 1.0 Hz target frequency. The target source parameters are fault location (x, y, and z coordinate), rise time, seismic moment, and moment tensors. Since strike, dip and rake angle were initially found to be less sensitive to affect the seismic wave as compared with other source parameters, moment tensors which are derived from these fault parameters are used as a target parameter. The input moment tensors to each node for a point source inside a cubic element, are given as follows[19].

$$M_{11} = -M_0(\sin\delta\cos\lambda\sin 2\phi + \sin 2\delta\sin\lambda\sin^2\phi)$$

$$M_{22} = M_0(\sin\delta\cos\lambda\sin 2\phi - \sin 2\delta\sin\lambda\cos^2\phi)$$

$$M_{33} = M_0(\sin 2\delta\sin\lambda) = -(M_{11} + M_{22})$$

$$M_{12} = M_0(\sin\delta\cos\lambda\cos 2\phi + \frac{1}{2}\sin 2\delta\sin\lambda\sin 2\phi)$$

$$M_{13} = -M_0(\cos\delta\cos\lambda\cos\phi + \cos 2\delta\sin\lambda\sin\phi)$$

$$M_{23} = -M_0(\cos\delta\cos\lambda\sin\phi - \cos 2\delta\sin\lambda\cos\phi)$$

$$M_{21} = M_{12}$$

$$M_{31} = M_{13}$$

$$M_{32} = M_{23}$$

Therein, ϕ, δ, λ and M_0 are strike angle, dip angle, rake angle, and seismic moment, respectively.

The model considered is a horizontally-layered model as shown in **Fig. 3**a), and the size of domain is 14.4 × 14.4 × 12km. The settings of synthetic model and observation points are shown in **Table 3** and **Fig. 3**b), respectively. The settings of synthetic model are shown in **Table 3**).

The multiscale approach is applied, and the solution which guarantee accuracy of 1.0 Hz is solved in a stepwise manner by the minimization of Eq.(6) for target frequencies of 0.25 Hz, 0.5 Hz, and 1.0 Hz.

In this analysis, 3 numerical experiments were carried out.

1) Fault location (x, y, and z coordinate) is estimated as rise time, seismic moment, and moment tensors are known;

2) Rise time and seismic moment are estimated simultaneously as other parameters are known;

3) Moment tensors are estimated as other parameters are known.

In the moment tensor inversion, since M_{33}=-(M_{11}+M_{22}), M_{12}=M_{21}, M_{13}=M_{31}, M_{23}=M_{32}, only 5 components, M_{11}, M_{22}, M_{12}, M_{13} and M_{23} are needed to be solved.

Initial solution, inversion result, and reference solution in each fault inversion are shown in **Table 4**, **Table 5**, and **Table 6**. The minimization of the objective function for each problem is shown in **Fig. 4**.

It can be observed that the fault location problem converges gradually to the reference solution as resolution of the synthetic model becomes higher. This result suggests that the accuracy of fault location inversion can be improved in the estimation by using high-resolution model. Meanwhile, rise time, seismic moment, and moment tensors have already converged to the reference solution in the low-resolution model of approximately 0.25 Hz target frequency.

In this application example, we considered a point source in the inversion analysis. Since we are using linear elastic formulation, extension to fault plane rupture is expected to be straightforward. This is because the resulting surface waveform of a fault plane rupture can be modeled as a superposition of surface waveforms caused by each point source in the fault plane. However, the computation time is expected to increase because the source parameters have to be estimated for all the point sources considered.

Our results show that the proposed inversion scheme can be applied to improving the accuracy of these source parameters, given that the accuracy of the crust model is guaranteed in the same target frequency. In the future, we seek to improve the rate of convergence by performing analysis on the appropriate objective function and waveform components (displacement, velocity, or acceleration, time-frequency misfit). Moreover, application to actual data would necessitate the use of regularization on the objective function or in the inversion procedure.

4. Conclusion

To improve the source parameter data to accurately reproduce waveforms in higher frequencies, a combined MCFEM and a multiscale inversion method is proposed. We emphasized the accuracy of computed synthetics in this inversion scheme, and demonstrated the applicability of MCFEM by a reproduction of an observed ground motion. In the inversion, we performed simple tests on each source parameter to determine their behavior in the minimization and to check the effectiveness of the multiscale approach. The results obtained show the applicability of the proposed method for improving source parameter given an accurate velocity structure.

In the future, we aim to improve the estimation accuracy of source parameters, as well as the convergence performance. Moreover, we intend to integrate the method proposed in the reference[1)] and the method proposed in this paper to formulate a simultaneous inversion method that includes all fault parameters, crust structure, and model constraints. Then, using this simultaneous inversion method, a specific target region will be chosen to check the applicability for estimating the crust structure and source parameters with high accuracy.

References

1) Quinay, P.E., Ichimura, T., Hori, M.: Development of a Forward-Inversion Crust Modeling Scheme for Accurate Strong-Ground Motion Prediction, *Proceedings of the 7th CUEE and 5th ICEE Joint Conference*, Tokyo, Japan, March 3-5, 2010.

2) H18. Working Paper of Special Project for Earthquake Disaster Mitigation in Urban Areas, *Ministry of Education, Culture, Sports, Science and Technology,* 2006, http://www.eri.u-tokyo.ac.jp/

3) Koketsu, K., Miyake, H., Afnimar and Tanaka, Y.: A Proposal for a Standard Procedure of Modeling 3-D Velocity Structures and its Application to the Tokyo Metropolitan Area, Japan, *Tectonophysics*, 472, pp. 290–300, 2009.

4) Graves, K., Wald, D.: Resolution analysis of finite fault source inversion using one- and three-dimensional Green's functions 1. Strong motions *Journal of Geophysical Research*, vol.106, no. B5, pp. 8745-8766, 2001.

5) Nozu, A., Irikura, K.: Strong-motion generation areas of a great subduction-zone earthquake: waveform inversion with empirical Green's functions for the 2003 Tokachi-oki earthquake *Bulletin of Seismological Society of America*, vol.98, no.1, pp. 180-197, 2008.

6) Zhao, L., Helmberger, D.V.: Source Estimation from Broadband Regional Seismograms, *Bulletin of the Seismological Society of America*, Vol.84, no.1, pp. 91-104, 1994.

7) Ichimura,T., Hori, M., Bielak, J.: A Hybrid Multiresolution Meshing Technique for Finite Element Three-Dimensional Earthquake Ground Motion Modelling in Basins Including Topog-

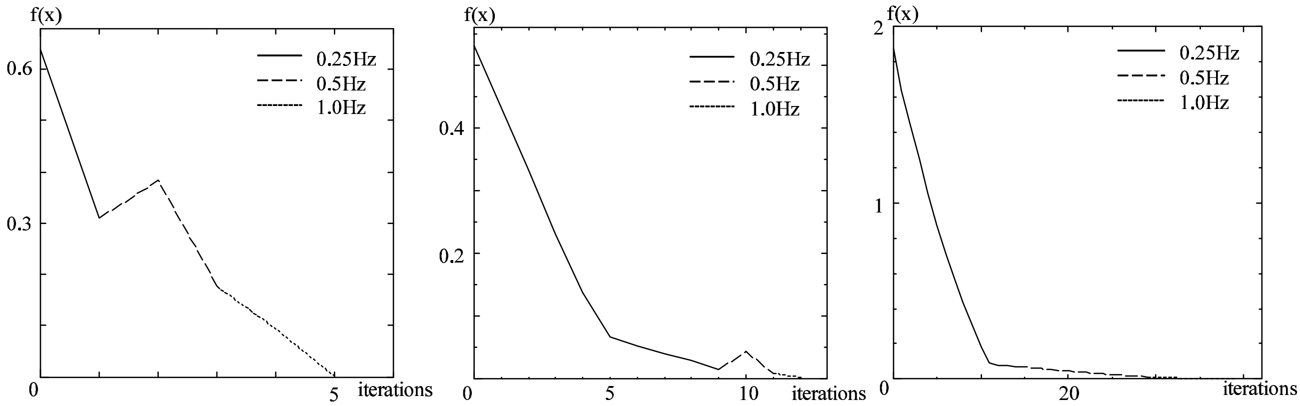

a) fault location   b) rise time and seismic moment   c) moment tensor

Fig. 4 Minimization of the objective function in the source parameter inversion. The unit values in the vertical axis is (m-sec.).

raphy, *Geophysical Journal International*, pp. 1221–1232, 2009.

8) Lysmer, J., and Kuhlemeyer, R. L.: Finite Dynamic Model for Infinite Media, *Proceedings of the American Society of Civil Engineers. Journal of the Engineering Mechanics Division*, Vol.95, No.EM4, pp. 859–877, 1969.
9) Cerjan, C., Kosloff, D., Kosloff, R., Reshef, M.: A nonreflecting boundary condition for discrete acoustic and elastic wave equations, *Geophysics*, vol.50, no.4, pp. 705–708, 1985.
10) K-net Kyoshin Network, Broadband Seismograph Network, Japan National Research Institute for Earth Science and Disaster Prevention, http://www.k-net.bosai.go.jp
11) F-net Broadband Seismograph Network, Japan National Research Institute for Earth Science and Disaster Prevention, http://www.fnet.bosai.go.jp/freesia/
12) Kikuchi, M., Ishida, M.: Source Retrieval for Deep Local Earthquake with Broadband Records, *Bulletin of the Seismological Society of America*, Vol.83, no.6, pp. 1855–1870, 1993.
13) Tanaka Y., Miyake, H., Koketsu, K., Furumura, T., Hayakawa, T., Baba, T., Suzuki, H., and Masuda, T.: The DaiDaiToku Integrated Model of the Velocity Structure beneath the Tokyo Metropolitan Area (2), *Abstracts the Japan Geoscience Union Meeting*, S116–P014, 2006.
14) Suzuki, W., Iwata, T.: Broadband seismic wave radiation process of the 2000 western Tottori, Japan, earthquake revealed from wavelet domain inversion *Journal of Geophysical Research*, vol.114, no. B08302, 2009.
15) Goto, H., Sawada, S.: Dynamic source inversion based on stable formulation and on identification of the resolution level via a multiscale approach. *Geophysical Journal International*, 167, pp. 779-793, 2005.
16) Koketsu, K., Miyake, H.: A Seismological Overview of Long-period Ground Motion. *Journal of Seismology*, 12: 133-143, 2008.
17) Nocedal, J.: Theory of Algorithms for Unconstrained Optimization, *Acta Numerica*, 1. pp. 199–242, 1992.
18) T. Aoyama, K. Shiono, S. Masumoto, T. Noto, Optimal Determination of Discontinuous Surfaces, *Geoinformatics*, vol.8, no.3, pp. 157-175, 1997.
19) Aki, K., Richards, P.: *Quantitative Seismology: Theory and Methods; Vol.1*, WH Freeman, New York,, 1980.
20) Graves, R.: Simulating Seismic Wave Propagation in 3D Elastic Media using Staggered-grid Finite-Differences. *Bulletin of Seismological Society of America*, Vol.86 No.4. pp.1091-1106, 1996
21) Koketsu, K., Fujiwara, H., Ikegami, Y.: Finite Element Simulation of Seismic Ground Motion with a Voxel Mesh. *Pure and Applied Geophysics*, Vol.161, pp.2183-2198, 2004.
22) Satoh, T., Kawase, H., Sato, T., Pitarka, A,: Three-Dimensional Finite-Difference Waveform Modeling of Strong Motions Observed in the Sendai Basin, Japan, *Bulletin of Seismological Society of America*, Vol.91,4,pp. 812-825, 2001.
23) Bielak, J.,Ghattas, O., Kim, E. J.: Parallel Octree-based Finite Element Method for Large-Scale Earthquake Ground Motion Simulation. *Computer Modeling in Engineering and Sciences*, Vol.10, pp.99-112, 2005.
24) Ji, C., Helmberger, D., Wald, D.: Basin Structure Estimation by Waveform Modeling: Forward and Inverse Method, *Bulletin of Seismological Society of America*, Vol.90,4,pp. 964-976, 2000.

25) Aoi, S.: Boundary Shape Waveform Inversion for Estimating the Depth of Three Dimensional Basin Structures, *Bulletin of Seismological Society of America*, Vol.92, pp. 2410-2418, 2002.
26) Earthquake Working Group Reports, Central Disaster Management Council, The 12th material, 2004, http://www.bousai.go.jp/jishin/chubou/shutochokka/12/shiryo2-2.pdf
27) Yamanaka, H., Furumura, T., Sato, H., Higashi, S., Shiba, Y., Sato, T., Hayakawa, T.: H18 Working Paper of Special Project for Earthquake Disaster Mitigation in Urban Areas, *Ministry of Education, Culture, Sports, Science and Technology*, pp. 486-514, 2006.

(Received March 9, 2010)